J. metamorphic Geol., 2005, **23,** 45–61 doi:10.1111/j.1525-1314.2005.00561.x

Discrete ultrahigh-pressure domains in the Western Gneiss Region, Norway: implications for formation and exhumation

D. B. ROOT[1], B. R. HACKER[1], P. B. GANS[1], M. N. DUCEA[2], E. A. EIDE[3] AND J. L. MOSENFELDER[4]
[1]*Department of Geological Sciences, UC Santa Barbara, Santa Barbara, CA 93106, USA (rootd@si.edu)*
[2]*Department of Geosciences, University of Arizona, Tucson, AZ 85721, USA*
[3]*Geological Survey of Norway, Leiv Erikssons vei 39, 7491 Trondheim, Norway*
[4]*Division of Geological and Planetary Sciences, California Institute of Technology, Pasadena, CA 91125, USA*

ABSTRACT New eclogite localities and new $^{40}Ar/^{39}Ar$ ages within the Western Gneiss Region of Norway define three discrete ultrahigh-pressure (UHP) domains that are separated by distinctly lower pressure, eclogite facies rocks. The sizes of the UHP domains range from *c.* 2500 to 100 km^2; if the UHP culminations are part of a continuous sheet at depth, the Western Gneiss Region UHP terrane has minimum dimensions of *c.* 165 × 50 × 5 km. $^{40}Ar/^{39}Ar$ mica and K-feldspar ages show that this outcrop pattern is the result of gentle regional-scale folding younger than 380 Ma, and possibly 335 Ma.The UHP and intervening high-pressure (HP) domains are composed of eclogite-bearing orthogneiss basement overlain by eclogite-bearing allochthons. The allochthons are dominated by garnet amphibolite and pelitic schist with minor quartzite, carbonate, calc-silicate, peridotite, and eclogite. Sm/Nd core and rim ages of 992 and 894 Ma from a 15-cm garnet indicate local preservation of Precambrian metamorphism within the allochthons. Metapelites within the allochthons indicate near-isothermal decompression following (U)HP metamorphism: they record upper amphibolite facies recrystallization at 12–17 kbar and *c.* 750 °C during exhumation from mantle depths, followed by a low-pressure sillimanite + cordierite overprint at *c.* 5 kbar and *c.* 750 °C. New $^{40}Ar/^{39}Ar$ hornblende ages of 402 Ma document that this decompression from eclogite-facies conditions at 410–405 Ma to mid-crustal depths occurred in a few million years. The short timescale and consistently high temperatures imply adiabatic exhumation of a UHP body with minimum dimensions of 20–30 km. $^{40}Ar/^{39}Ar$ muscovite ages of 397–380 Ma show that this extreme heat advection was followed by rapid cooling (*c.* 30 °C Myr^{-1}), perhaps because of continued tectonic unroofing.

Key words: $^{40}Ar/^{39}Ar$; cordierite; eclogite; Norway; thermobarometry; ultrahigh pressure.

INTRODUCTION

The Scandinavian Caledonides, formed during the Silurian continental collision of Baltica and Laurentia, contain one of the world's largest ultrahigh-pressure (UHP) terranes in the Western Gneiss Region (WGR) of Norway. Metamorphic pressures in this *c.* 50 000 km^2 basement culmination in the core of the Caledonian orogen reached *c.* 40 kbar, producing coesite on a regional scale. Understanding the genesis and exhumation of these remarkable rocks sheds light on numerous large-scale geodynamic and geochemical processes, including continental collisions and the recycling of continental material into the mantle.

This study addresses two important issues regarding the formation and exhumation of the UHP rocks in the WGR: (i) the size, shape, and structure of the UHP terrane; and (ii) the structural and petrological relationship between the UHP rocks and overlying allochthonous schists and gneisses –including their *P–T–*time paths. Geochronology, petrology and structural geology are used to demonstrate that the UHP rocks are exposed in three separate antiformal domains, separated by high-pressure (HP) rocks, that in aggregate define a UHP terrane with minimum average dimensions of *c.* 165 × 50 × 5 km. The distribution of eclogites suggests that the allochthons and basement were juxtaposed prior to the UHP–HP metamorphism and shared the same subduction and exhumation history. New $^{40}Ar/^{39}Ar$ ages in conjunction with existing geochronology show that the rocks were exhumed from UHP mantle depths to shallow crustal levels in 5–10 Myr.

Present address: D. B. Root, Department of Mineral Sciences, National Museum of Natural History, Washington, DC 20560-0119, USA.

NEW UHP ECLOGITES AND THE SIZE AND SHAPE OF THE UHP DOMAINS

The UHP rocks of Norway are exposed in the coastal reaches of the Western Gneiss Region (WGR), between Nordfjord in the south to Fjørtoft in the north (Fig. 1); high-pressure rocks extend over a much greater area to the north, east and south (Cuthbert

© 2005 Blackwell Publishing Ltd

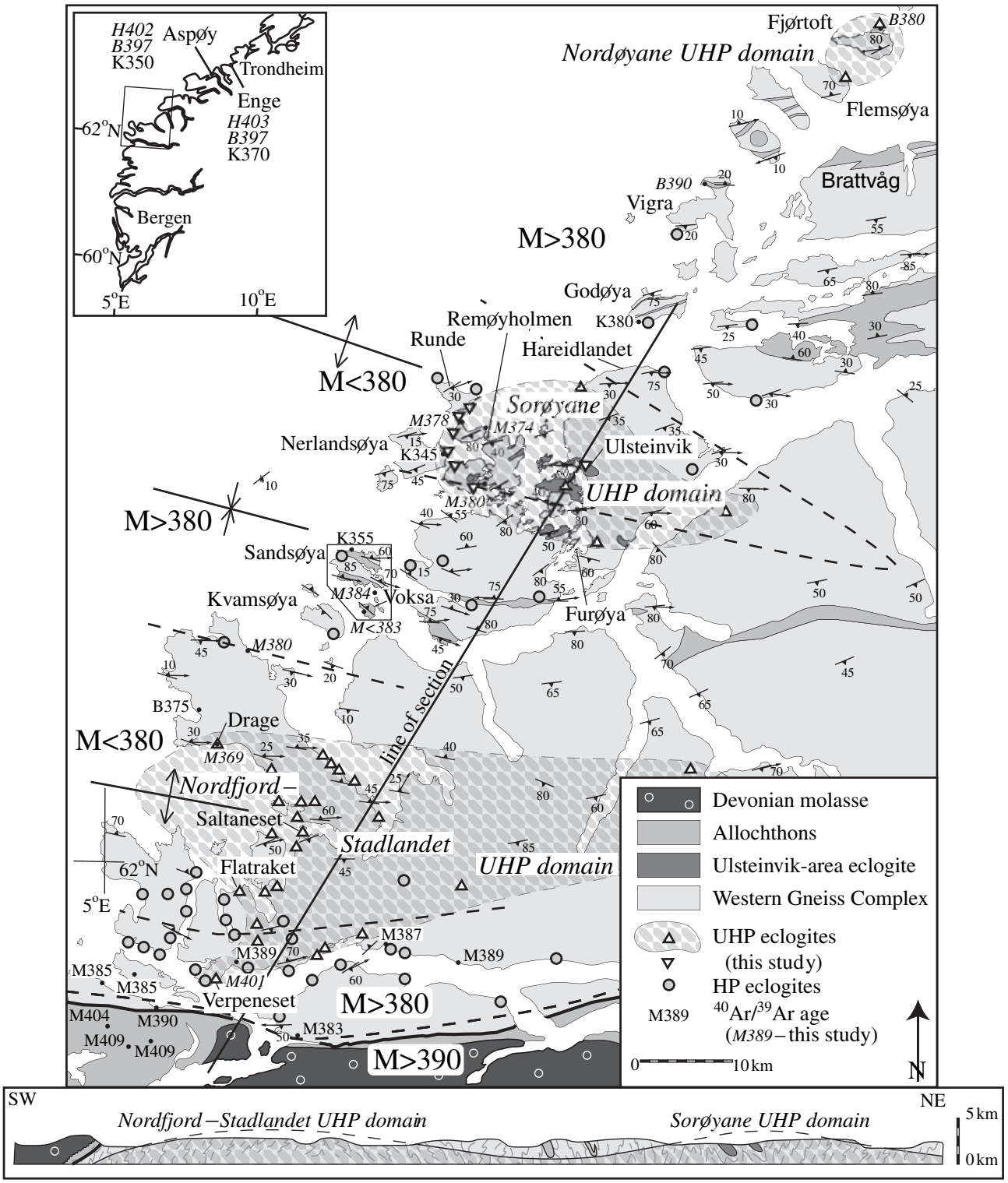

Fig. 1. Map of the study area, showing the ultrahigh-pressure domains exposed in culminations beneath the high-pressure domains. $^{40}Ar/^{39}Ar$ ages denoted as B, biotite; H, hornblende; K, K-feldspar (from Hacker *et al*., 2004); M, muscovite; ages from this study are in italics. Other ages from Chauvet & Dallmeyer (1992); Andersen *et al*. (1998) and Lux (1985). Geology based in part on Tveten *et al*. (1998a,b) and Krabbendam & Wain (1997).

© 2005 Blackwell Publishing Ltd

et al., 2000; Walsh & Hacker, 2004). Most of the UHP–HP terrane consists of continental orthogneisses overlain locally by chiefly paragneisses. Dispersed eclogites blocks that make up only *c.* 1 vol.% of the terrane contain nearly all the evidence of former ultrahigh pressures, in the form of coesite, diamond and other high-pressure minerals. Both the eclogites and the host gneisses experienced a strong amphibolite facies recrystallization and deformation following the UHP event. Although the eclogites locally survived this overprint, nearly all UHP minerals and structures that might have existed in the host gneisses were obliterated and replaced by amphibolite-facies parageneses, gently E- and W-plunging lineations, and N- and S-dipping foliations isoclinally folded about shallowly E- and W-plunging axes (Fig. 1).

It was in the Nordfjord–Stadlandet region where UHP eclogites were first recognized, based on the presence of coesite (Smith, 1984). Since then, *c.* 30 eclogite localities containing either coesite or polycrystalline quartz pseudomorphs after coesite have been identified, delineating a *c.* 2500 km^2 region named the Nordfjord–Stadlandet UHP domain (Wain, 1997; Cuthbert *et al.*, 2000). UHP eclogites were subsequently identified more than 125 km to the north on Fjørtoft (Terry *et al.*, 2000a) and > 50 km to the east (Walsh & Hacker, 2004), suggesting that the Norwegian UHP terrane might approach 10 000 km^2.

To evaluate the size and structure of the UHP terrane, this study focused on the Sorøyane (the 'Southern Islands', from Kvamsøya to Runde), that lie between the Nordfjord–Stadlandet and Fjørtoft UHP domains (Fig. 1). Eclogites are reasonably widespread in the study area, permitting the boundaries of the UHP terrane to be mapped on the basis of the presence or absence of coesite or coesite pseudomorphs. This study identified seven new UHP eclogites (Fig. 1) by the discovery of polycrystalline quartz inclusions within garnet and omphacite. Relict coesite (Fig. 2) was identified in the core of one such inclusion from an eclogite on Runde (Fig. 1). Conventional thermobarometry is impossible in most of these eclogites because of the absence of phengite and kyanite, but Krogh Ravna (in Carswell *et al.*, 2003a) reported a pressure of 32 kbar at 795 °C from eclogite on the nearby island of Furøya (Fig. 1), and the presence of former coesite requires pressures of at least 28 kbar in all the other UHP eclogites. Additional new findings include dozens of other eclogites lacking evidence of UHP metamorphism. As is clear from Fig. 1, the Sorøyane UHP localities are geographically distinct from those farther north and south, and separated from those localities by distinctly low-pressure (though still high-pressure) rocks. These data, in conjunction with eclogite locales studied by Cuthbert *et al.* (2000), define three distinct UHP domains along the Norwegian coast: the 'Nordfjord–Stadlandet UHP domain' with an outcrop area of *c.* 2500 km^2, the 'Sorøyane UHP domain' of *c.* 1000 km^2, and the 'Nordøyane UHP domain' of *c.* 100 km^2 (Fig. 1). The delineation of these UHP domains based on the observation of coesite or relict coesite in eclogites is limited by two main factors: eclogites must be present, coesite must have formed, and it must be preserved. Unfortunately, eclogites are uncommon in certain rock types and the formation and preservation of coesite require favourable circumstances that did not always occur. Despite this limitation, the geochronological data presented below show that these three UHP domains are likely connected at depth and define a UHP terrane with minimum average dimensions of *c.* 165 × 50 × 5 km.

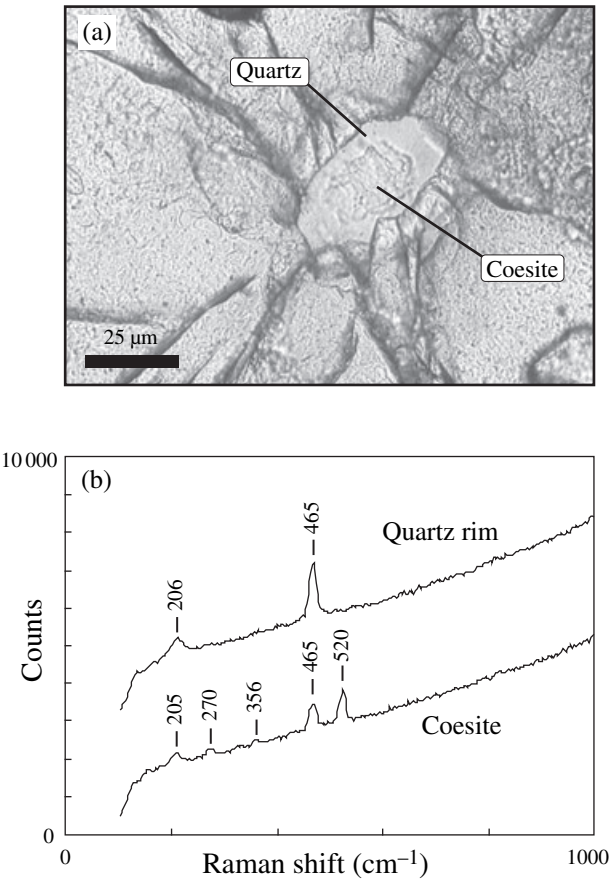

Fig. 2. (a) Relict coesite in core of polycrystalline quartz inclusion within garnet, eclogite R9824C, Runde; transmitted, plane-polarized light image. (b) Raman spectrum from quartz rim and coesite core of same inclusion; peak at 525 cm^{-1} is diagnostic of coesite.

ALLOCHTHONOUS SEQUENCES WITHIN THE WGR

The main unit within the WGR, the Western Gneiss Complex (WGC), consists chiefly of *c.* 1700–950 Ma tonalitic to granodioritic orthogneisses (Corfu, 1980; Schärer, 1980; Tucker *et al.*, 1990) considered to be Baltica basement. Overlying successions of more volumetrically minor and lithologically more varied rocks

© 2005 Blackwell Publishing Ltd

are either the metamorphosed equivalents of sediments deposited on the basement (Schouenborg, 1988) or remnants of the Caledonian thrust nappes preserved in the foreland farther east (Bryhni, 1989). In particular, allochthons exposed in the foreland have been traced >200 km westward all the way across the WGR to the Nordøyane (Fig. 1) (Hernes, 1956; Rickard, 1985; Robinson, 1995; Terry *et al*., 2000a) and Nordfjord areas (Young *et al*., 2003; Walsh & Hacker, 2004). Determining whether these allochthonous successions and the WGC basement were juxtaposed prior to or after the UHP–HP metamorphism is crucial to unravelling how the UHP rocks were formed and exhumed. This question is best answered by comparing the pressure–temperature–time paths of the two units and by examining the structure of the basement–allochthon contact. The Sorøyane area affords an excellent opportunity to evaluate this question because of the presence of UHP eclogites, HP eclogites, and allochthonous metasedimentary and meta-igneous rocks.

In the northern Sorøyane, the most abundant rock is a medium- to fine-grained, well-foliated to massive orthogneiss that ranges in composition from quartz diorite to granite. Because of similarity in composition and fabric to the common orthogneiss of the WGC, this gneiss is inferred to represent Baltica basement. Eclogite blocks are relatively common locally within the gneiss. This basement gneiss is overlain(?) by rocks inferred to be allochthonous, based on correlation with the WSW–ENE-trending synclines of allochthonous rocks mapped and described farther northeast (e.g. at Brattvåg, Fig. 1) by Robinson (1995) and east of Fig. 1 by Walsh & Hacker (2004). Inferred allochthonous rocks within the study area include successions of quartzite, marble, calc-silicate gneiss, kyanite–garnet–biotite schist, very coarse grained K-feldspar augen gneiss, amphibolite, eclogite and peridotite; a few minor felsic plutons intrude these rocks.

The island of Remøyholmen (Fig. 3) is our best studied section of allochthonous rock in the northern Sorøyane. This tiny island is underlain by an *c*. 200-m thick, steeply S–SSE-dipping package of dominantly paragneisses and paraschists. The north side of the island consists of interlayered amphibolites, impure quartzites, marbles and pelitic schists. Variably deformed, undifferentiated anorthosites and gabbros crop out on the southeast side. A specific 20 m thick succession of impure quartzite, impure marble, kyanite–garnet–biotite schist, and a second impure marble is correlated with the Saetra and Blåhø Nappes described by Robinson (1995). Eclogites occur in some units (Fig. 3), none of which show evidence of UHP metamorphism. Contacts between the allochthonous sequence and the surrounding orthogneiss are, unfortunately, underwater.

The largest body of allochthonous rock in the northern Sorøyane is at Ulsteinvik (Fig. 1). There, a multi-kilometre scale UHP eclogite body is sheathed in garnet–biotite–kyanite schist, quartzite, marble (Mysen & Heier, 1972) and coarse augen gneiss, rock types herein correlated with the Blåhø and Risberget Nappes described by Robinson (1995). Because these nappes are allochthonous, the eclogite body is probably also allochthonous.

In the southern Sorøyane, on the islands from Sandsøya to Voksa (Fig. 4) rocks inferred by Gjelsvik (1951) to be basement consist of coarse-grained, dioritic, migmatitic, locally garnet-bearing quartzofeldspathic gneiss, anorthosite, minor gabbro, and scattered HP (not UHP) eclogites. Probable allochthonous rocks – again, based on lithological similarities

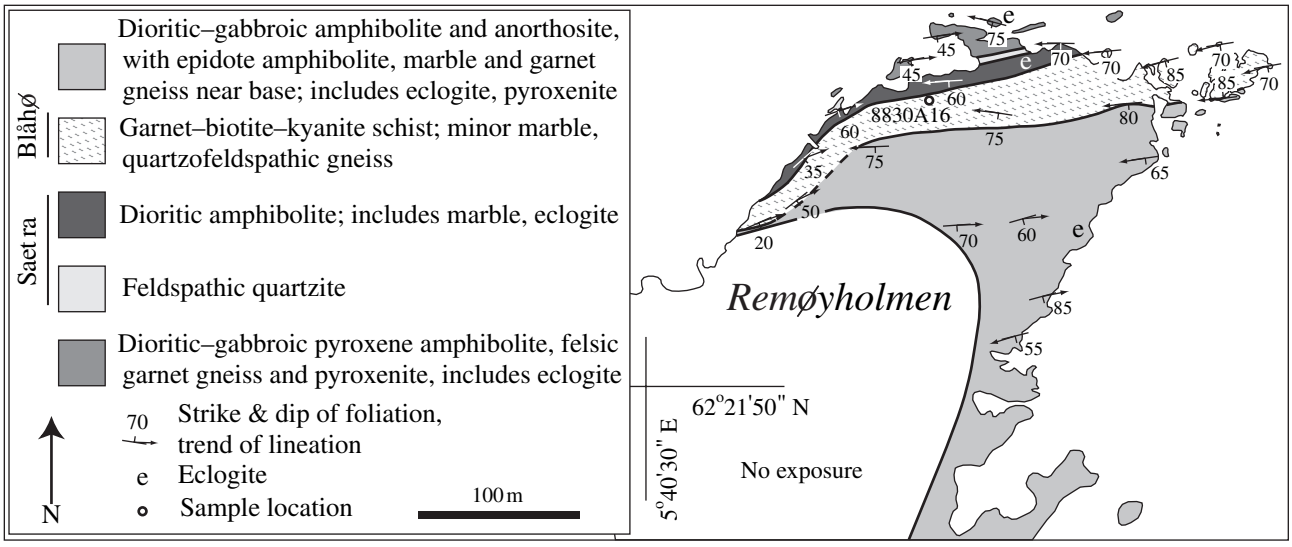

Fig. 3. Geological map of Remøyholmen, emphasizing the sequence inferred to be allochthonous based on correlation with rocks mapped by Robinson (1995).

© 2005 Blackwell Publishing Ltd

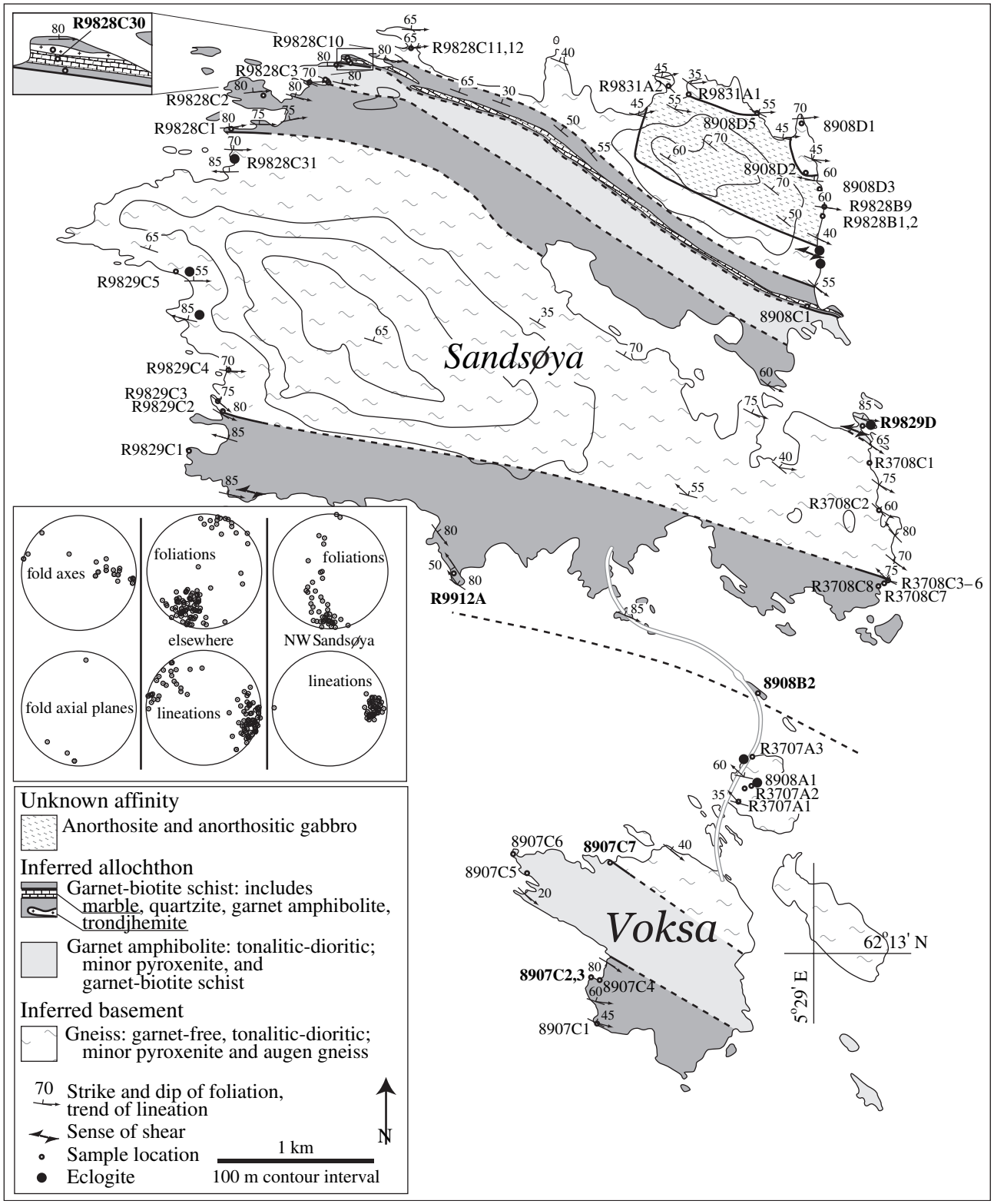

Fig. 4. Geological map of Sandsøya and Voksa, showing inferred allochthonous and basement rocks. Geology based in part on Lutro & Thorsnes (1990).

© 2005 Blackwell Publishing Ltd

with allochthonous rocks mapped by Robinson (1995) and Walsh & Hacker (2004) – consist mostly of banded diopside-bearing amphibolite and garnet–biotite schist, with less augen gneiss, granitic gneiss, feldspathic quartzite and marble. Extensive outcrops of anorthosite and anorthositic gabbro exposed on northeastern Sandsøya may be allochthonous or part of the basement. Boudins of pyroxenite and tonalitic to granodioritic melts are abundant within the allochthonous rocks, but eclogites have not been recognized. The contacts between the basement and allochthons are structurally concordant – nowhere marked by significant faults or shear zones – and were mapped solely on the basis of rock type. Locally, however, in contrast to the northern Sorøyane, the distinction between rocks mapped as basement and allochthon is equivocal. For instance, on SE Sandsøya the contact between the garnet-bearing gneiss inferred to be basement and the garnet–biotite–kyanite schist inferred to be allochthonous is gradational in composition. It remains possible that all the rocks on these islands are allochthonous; indeed, some of the rock types delineated as basement in this study have elsewhere been mapped as allochthonous (Bryhni, 1989). Regardless, no UHP eclogites have been identified in the southern Sorøyane.

Thus, the Sorøyane includes a northern UHP domain characterized by a basement that contains UHP eclogites overlain by allochthons that locally contain UHP eclogites. The southern HP part of the Sorøyane is characterized by a basement that contains HP eclogites overlain by allochthons that are not known to contain eclogites and by possibly allochthonous rocks that do contain HP eclogites. The contact between the UHP and HP domain is diffuse and defined solely on the presence or absence of UHP eclogites; indeed, extant petrological and structural data permit this 'contact' between UHP and HP to reflect a smooth gradient in pressure. The allochthon/basement contacts – though locally marked by sharp changes in rock type – are also devoid of faults or shear zones.

PETROLOGY AND THERMOBAROMETRY OF ALLOCHTHON PELITES

Following the UHP–HP metamorphism, all the units subsequently experienced a high-pressure amphibolite facies and a low-pressure granulite facies overprint. To understand this metamorphic evolution, thermobarometry was conducted on four kyanite-bearing, metapelitic samples from allochthonous supracrustal rocks on Sandsøya, Voksa and Remøyholmen (Fig. 1). All samples contain garnet, kyanite, sillimanite, biotite, plagioclase and quartz. Staurolite is present in three samples, and cordierite or pseudomorphs after cordierite occurs in two samples. Notably absent from all samples are muscovite and K-feldspar.

Electron microprobe data are shown in Table 1, with ferric iron determined by charge balance; *P–T* determinations are summarized in Table 2. Temperatures and pressures were calculated chiefly with the garnet–biotite Fe/Mg exchange equilibrium (GARB) and the garnet–kyanite/sillimanite–quartz–plagioclase equilibrium (GASP), using THERMOCALC version 3.1 (Powell *et al.*, 1998); this was supplemented as necessary with other equilibria calculated by THERMOCALC and by phase stability considerations. Thermobarometry in these high-temperature pelites is complicated by a number of factors. All biotite is homogeneous or weakly zoned, implying erasure of growth zoning. About half the analysed garnet has flat or nearly flat Mg# and X_{sps} profiles indicative of diffusional homogenization (Fig. 5a). Other garnet shows a rimward decrease in X_{grs} suggesting decompression, and an increase in Mg# and decrease in X_{sps} indicative of prograde growth (Fig. 5b), but even these apparently prograde-zoned garnet show evidence of diffusional smoothing: X_{sps} in garnet cores never exceeds rim values by more than a factor of four.

All garnet was also affected by resorption, and has embayed margins typically fringed by biotite (Fig. 6a). Sharp increases in X_{sps} within 50–350 μm of garnet rims are inferred to represent substantial resorption; concomitant decreases in Mg# and X_{grs} imply that the resorption was the result of net-transfer reactions during decompression and cooling (Fig. 5a,b). The effects of this resorption on the modes and compositions of garnet and biotite were modelled, following Kohn & Spear (2000), but temperatures derived from this method are imprecise, and considered unreliable (Fig. 7). Better constraints on peak temperatures were derived from phase stability considerations discussed below.

Pressures at peak temperature were estimated from the grossular content of garnet just inside the resorption-induced rim and from the rim composition of matrix plagioclase. Pressures during garnet core formation, determined from garnet and plagioclase core compositions, are *c.* 2–4 kbar higher. In all samples, these core pressures are minima because the diffusion implied by the shape of the garnet zoning profiles likely reduced X_{grs} even in the core of the largest garnet.

SANDSØYA AND VOKSA

Three pelitic samples from Sandsøya and Voksa (R9828C30, R9912A & 8907C7) (Fig. 4) exhibit a peak assemblage of kyanite + garnet + biotite + plagioclase + quartz. Muscovite is also assumed to have been present at this stage, and to have subsequently broken down during the HT/LP overprint evident from the presence of late sillimanite in all samples, cordierite in R9828C30 (Fig. 8a), and pinite after cordierite in 8907C7 (Fig. 6b). Temperatures derived from garnet–biotite Fe–Mg exchange vary among the three samples (Table 2, Fig. 7), and are not considered reliable, but temperatures of *c.* 650–800 °C are indicated by the assemblage garnet + kyanite + biotite. All three

© 2005 Blackwell Publishing Ltd

© 2005 Blackwell Publishing Ltd

Table 1. Electron microprobe analyses.

Sample	SiO_2	TiO_2	Al_2O_3	Cr_2O_3	Fe_2O_3	FeO	MnO	MgO	CaO	Na_2O	K_2O	Total	#O	Si	Ti	Al	Cr	Fe^{3+}	Fe^{2+}	Mn	Mg	Ca	Na	K	Sum	X_{An}	Mg#	X_{Sps}	X_{Grs}
8830A16																													
Grt																													
Core	38.41	0.08	21.24	0.06	0.97	23.13	1.53	6.30	7.88	<	<	99.6	12	2.99	0.01	1.95	0.00	0.06	1.51	0.10	0.73	0.66	<	<	8.00		0.33	0.03	0.22
Trough	39.25	0.05	21.58	0.07	0.02	25.05	0.76	8.27	5.01	<	<	100.1	12	3.02	0.00	1.96	0.00	0.00	1.61	0.05	0.95	0.41	<	<	8.00		0.37	0.02	0.14
Bt	36.85	2.93	17.75	0.18	n.d.	12.37	<	15.44	<	0.05	9.32	94.9	11	2.72	0.16	1.54	0.01	n.d.	0.76	<	1.70	<	0.01	0.88	7.78		0.69		
Pl																													
Core	64.62	<	22.38	<	<	n.d.	<	<	3.41	9.70	0.06	100.2	8	2.84	<	1.16	<	<	n.d.	<	<	0.16	0.83	0.00	4.99	0.16			
Rim	62.07	<	24.17	<	<	n.d.	<	<	5.58	8.52	0.08	100.4	8	2.74	<	1.26	<	<	n.d.	<	<	0.26	0.73	0.01	5.00	0.27			
8907C7																													
Grt																													
Core	37.56	<	21.25	<	0.23	27.80	1.76	4.82	5.26	<	<	98.7	12	2.99	<	2.00	<	0.01	1.85	0.12	0.57	0.45	<	<	8.00		0.24	0.04	0.15
Trough	38.14	0.08	21.73	<	n.d.	27.62	0.34	6.92	4.14	<	<	99.0	12	2.99	0.01	2.01	<	n.d.	1.81	0.02	0.81	0.35	<	<	8.00		0.31	0.01	0.12
Bt	36.43	1.85	18.23	0.13	2.40	12.26	<	14.55	<	0.36	8.52	94.7	11	2.70	0.10	1.59	0.01	0.13	0.76	<	1.61	<	0.05	0.81	7.76		0.68		
Pl																													
Core	63.57	<	22.94	<	<	n.d.	<	<	4.14	9.22	0.19	100.1	8	2.81	<	1.19	<	<	n.d.	<	<	0.20	0.79	0.01	5.00	0.20			
Rim	60.37	<	25.07	<	0.07	n.d.	<	<	6.30	8.14	<	100.0	8	2.69	<	1.32	<	0.00	n.d.	<	<	0.30	0.70	0.00	5.01	0.30			
R9828C30																													
Grt																													
Core	38.14	<	21.92	0.06	2.12	23.89	1.04	7.76	5.33	<	<	100.3	12	2.94	<	1.99	0.00	0.12	1.54	0.07	0.89	0.44	<	<	8.00		0.37	0.02	0.15
Trough	38.04	<	21.97	<	2.18	25.35	0.66	8.27	3.69	<	<	100.2	12	2.94	<	2.00	<	0.13	1.64	0.04	0.95	0.31	<	<	8.00		0.37	0.01	0.10
Bt	36.70	2.18	17.23	0.11	2.15	12.27	0.05	14.90	<	0.34	8.63	94.6	11	2.73	0.12	1.51	0.01	0.12	0.76	0.00	1.65	<	0.05	0.82	7.77		0.68		
Pl																													
Core	61.86	<	24.00	<	0.09	n.d.	<	<	5.42	8.59	0.09	100.1	8	2.74	<	1.25	<	0.00	n.d.	<	<	0.26	0.74	0.01	5.00	0.26			
Rim	59.33	<	25.14	<	0.17	n.d.	<	<	6.74	7.76	0.07	99.2	8	2.67	<	1.33	<	0.01	n.d.	<	<	0.32	0.68	0.00	5.01	0.32			
Crd	49.08	<	33.58	<	1.08	3.88	0.10	10.78	<	0.20	<	98.7	18	4.95	<	4.00	<	0.08	0.33	0.01	1.62	<	0.04	<	11.03		0.80		
St	26.33	0.30	53.79	0.20	n.d.	13.06	0.17	2.92	<	0.36	<	97.1	46	7.38	0.06	17.76	0.04	n.d.	3.06	0.04	1.22	<	0.20	<	29.76		0.28		
R9912A																													
Grt																													
Core	38.11	<	21.65	<	2.09	25.11	0.65	8.07	4.23	<	<	99.9	12	2.95	<	1.98	<	0.12	1.63	0.04	0.93	0.35	<	<	8.00		0.36	0.01	0.12
Trough	39.19	<	21.88	<	0.79	25.16	0.49	8.62	4.56	<	<	100.7	12	2.99	<	1.97	<	0.05	1.61	0.03	0.98	0.37	<	<	8.00		0.38	0.01	0.12
Bt	36.70	2.45	17.20	0.10	1.10	13.91	<	14.26	<	0.37	8.68	94.8	11	2.73	0.14	1.51	0.01	0.06	0.87	<	1.58	<	0.05	0.83	7.78		0.65		
Pl																													
Core	64.11	<	22.57	<	0.06	n.d.	<	<	3.79	9.42	0.13	100.1	8	2.83	<	1.17	<	0.00	n.d.	<	<	0.18	0.81	0.01	4.99	0.18			
Rim	62.00	<	24.23	<	0.16	n.d.	<	<	5.50	8.66	0.05	100.6	8	2.74	<	1.26	<	0.01	n.d.	<	<	0.26	0.74	0.00	5.00	0.26			
R9829D																													
Grt																													
Core	36.99	0.05	20.51	0.05	1.17	26.00	5.73	3.01	5.55	<	<	99.1	12	2.98	0.00	1.95	0.00	0.07	1.75	0.39	0.36	0.48	<	<	8.00		0.17	0.13	0.16
Rim	37.49	0.01	20.68	<	0.20	26.61	5.18	3.17	5.65	<	<	99.0	12	3.02	0.00	1.96	<	0.01	1.79	0.35	0.38	0.49	<	<	8.00		0.18	0.12	0.16
Bt (incl.)	35.55	4.02	18.12	0.04	n.d.	19.00	0.14	9.09	<	0.29	9.48	95.7	11	2.70	0.23	1.62	0.00	n.d.	1.20	0.01	1.03	<	0.04	0.92	7.75		0.46		
	35.51	3.82	16.97	0.04	n.d.	18.49	0.10	11.01	<	0.13	9.25	95.4	11	2.70	0.22	1.52	0.00	n.d.	1.17	0.01	1.25	<	0.02	0.90	7.78		0.51		
Ms (incl.)	45.57	0.34	33.26	0.05	2.87	1.75	0.11	0.85	0.06	0.62	10.17	95.7	11	3.06	0.02	2.63	0.00	0.15	0.10	0.01	0.09	0.00	0.08	0.87	7.01		0.46		
Pl (incl.)	53.68	<	28.74	<	0.34	n.d.	0.08	<	10.51	5.33	0.08	98.8	8	2.45	<	1.55	<	0.01	n.d.	0.00	<	0.51	0.47	0.01	5.01	0.52			
	46.09	<	33.78	<	0.31	n.d.	0.04	<	16.28	1.86	<	98.4	8	2.15	<	1.86	<	0.01	n.d.	0.00	<	0.81	0.17	<	5.00	0.83			

All analyses conducted at 15 kV and 15 nA.
The symbol '<' denotes below electron microprobe detection limit.
n.d., not determined.

Table 2. Themobarometry results.

Sample	Thermometer	Barometer	*T* (°C)	*P* (kbar)	Cor
8830A16					
Core	[Grt Ky Bt]*	Grs Ky Pl Qtz	(650–800)	14–17.5	n/a
Trough	*Grt Bt (1.8)*†	Grs Ky Pl Qtz	*785 ± 60*†	*13.7 ± 0.4*†	n/a
R9828C30					
Core	[Grt Ky Bt]	Grs Ky Pl Qtz	(650–800)	11.5–14.5	n/a
Trough	*Grt Bt (3.8)*	Grs Ky Pl Qtz	*725 ± 60*	*10.7 ± 0.5*	n/a
R9828C30	Grt Crd Sil Qtz	Intersection	727 ± 46	4.7 ± 0.3	0.74
R9912A					
Core	[Grt Ky Bt]	Grs Ky Pl Qtz	(650–800)	12–15	n/a
Trough	*Grt Bt (2.9)*	Grs Ky Pl Qtz	*880 ± 70*	*15.2 ± 0.5*	n/a
8907C7					
Core	[Grt Ky Bt]	Grs Ky Pl Qtz	(650–800)	12–15	n/a
Trough	*Grt Bt (2.7)*	Grs Ky Pl Qtz	*645 ± 50*	*9.9 ± 0.5*	n/a
R9829D	Grt Bt	Grt Bt Ms Pl	759 ± 77	8.6 ± 1.1	0.90

Uncertainties are 1σ.
Cor, correlation coefficient from THERMOCALC version 3.1 with May 2001 database (Holland & Powell, 1998).
*Listings in brackets represent stability fields.
†Estimates in italics use correction for retrograde net transfer reactions (Kohn & Spear, 2000); resulting biotite Mg# in parentheses.

samples yield nearly identical minimum peak pressures of *c*. 11.5–15 kbar within the kyanite stability field (Table 2), based on GASP equilibria derived from the core compositions of garnet and plagioclase (Fig. 9).

A quantitative estimate of the subsequent HT/LP metamorphic conditions in the Sandsøya/Voksa region can be made from sample R9828C30. Abundant cordierite + quartz ± magnetite intergrowths occur between garnet and biotite, and as patches and seams throughout the matrix, while rare cordierite + biotite + quartz inclusions occur near garnet rims (Fig. 8a). Equilibria among the most magnesian garnet rims, cordierite, sillimanite and quartz yield an estimate of 4.7 ± 0.3 kbar and 727 ± 46 °C (Table 2; Fig. 9). The addition of biotite to this assemblage has little effect on calculated pressure and temperature, while nearby plagioclase (An_{41}) is too albitic to be in equilibrium. These conditions overlap the cordierite stability field of average pelites (White *et al.*, 2001). One kyanite porphyroblast in this sample is partially replaced by sillimanite and subsequently by intergrown An_{90} plagioclase + Mg#29 staurolite + magnetite (Fig. 8b), indicating final retrogression through staurolite-stable conditions (Fig. 9).

Similar HT/LP metamorphism of sample 8907C7 is evident from the former presence of cordierite shown by abundant symplectites of pinite + quartz + magnetite surrounding biotite and garnet (Fig. 6b), as well as from thin pinite–quartz–sillimanite–magnetite seams throughout the matrix. Staurolite occurs in two textural types: large (> 100 μm) porphyroblasts near garnet and kyanite (Fig. 6b), and smaller (< 50 μm) porphyroblasts lying 50–100 μm from margins of resorbed garnet. The latter presumably grew during isobaric cooling following the granulite facies metamorphism, similar to staurolite in sample R9828C30.

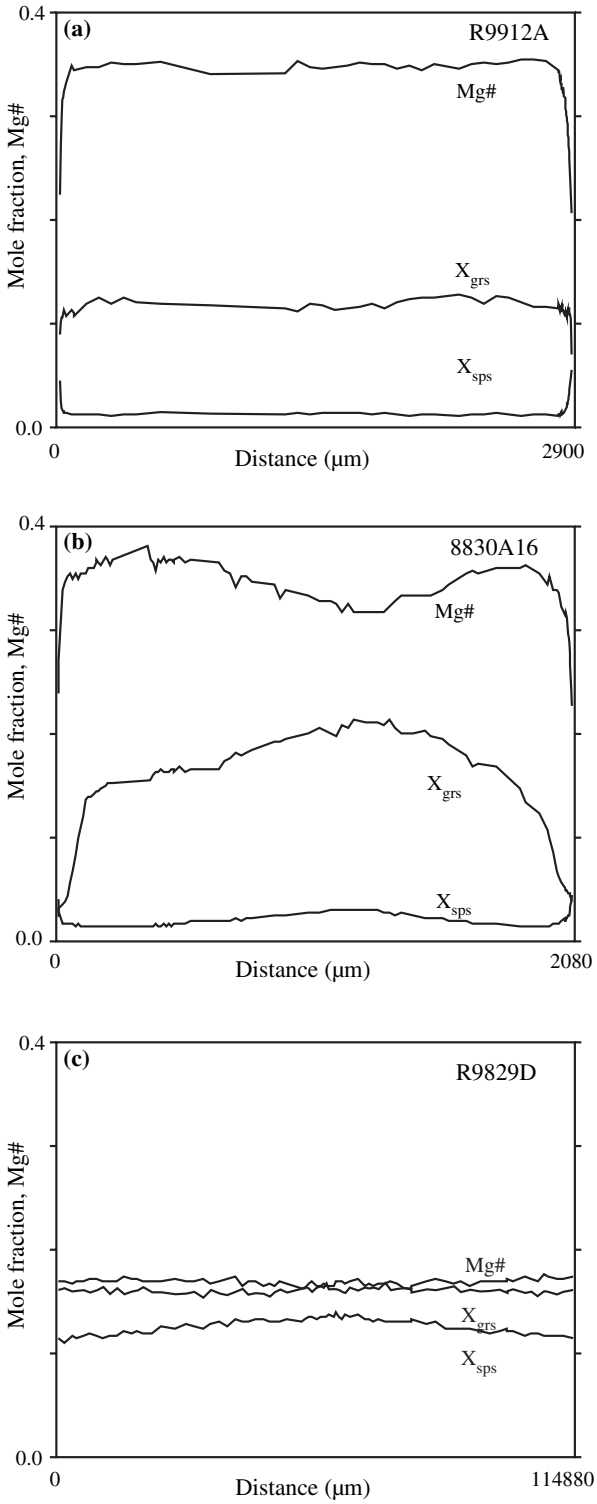

Fig. 5. Garnet major element profiles. Homogenization of growth zoning in smaller garnet is evident from completely flattened (a) and mostly flattened (b) X_{sps} profiles. Near-rim modification in (a) and (b) is because of garnet resorption during retrograde net-transfer reactions. (c) Weak bell-shaped X_{sps} zoning and lack of zoning of X_{grs} and Mg# reflect Proterozoic garnet growth under nearly constant pressure and temperature. Note different distance scale.

© 2005 Blackwell Publishing Ltd

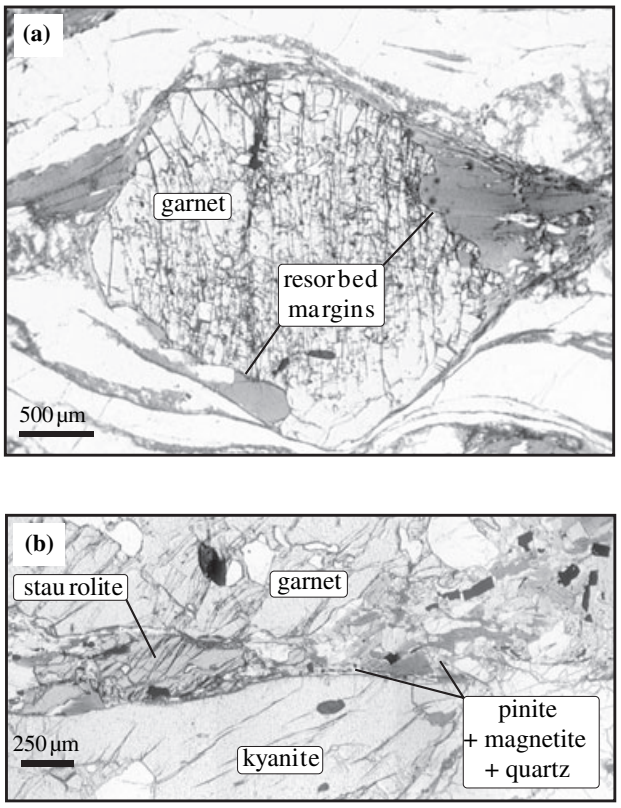

Fig. 6. Transmitted, plane-polarized light images of thin section textures. (a) 8830A16, garnet with embayments and fringing biotite because of resorption. (b) 8907C7, staurolite porphyroblast between kyanite and garnet and intergrowths of pinite (after cordierite), quartz and magnetite replacing biotite.

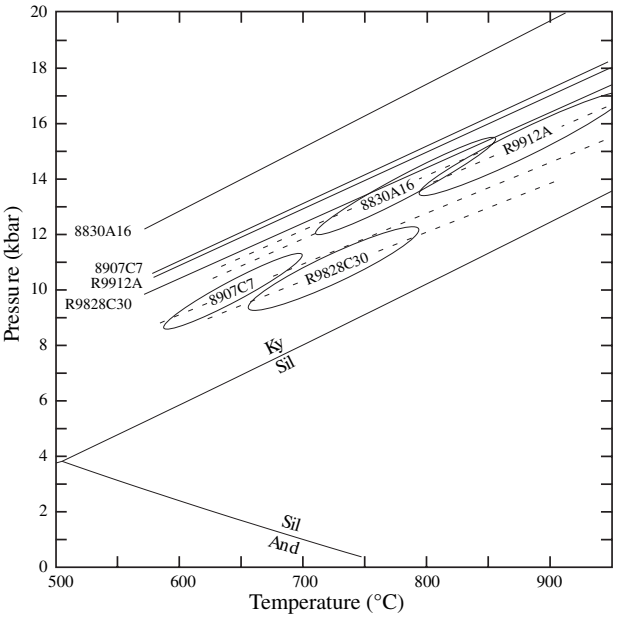

Fig. 7. Garnet–kyanite–quartz–plagioclase (GASP) barometry from garnet and plagioclase core compositions (solid lines; minimum estimate of peak pressure) and garnet Fe-trough + plagioclase rim compositions (dashed lines; estimate of conditions of completion of garnet growth). Ellipses represent 1σ uncertainties from THERMOCALC calculated by combining the latter with garnet–biotite (GARB) thermometry, using a biotite composition correction for retrograde garnet resorption.

REMØYHOLMEN

In contrast to pelites from Sandsøya and Voksa, sample 8830A16 from Remøyholmen (Fig. 3) lacks staurolite and cordierite, and yields a significantly higher minimum peak pressure of 14–17 kbar for temperatures of 650–800 °C (Fig. 9). Abundant late sillimanite and the absence of muscovite attest to subsequent decompression.

PRESSURE–TEMPERATURE SUMMARY

In combination, these four samples imply that the allochthons in the Sorøyane experienced a regional upper amphibolite facies metamorphism at *c.* 650–800 °C and >12–17 kbar (Fig. 9). This high-pressure amphibolite facies metamorphism was followed by apparent isothermal decompression to granulite facies conditions, *c.* 5 kbar, evident from late sillimanite growth and the absence of muscovite in all samples, and from cordierite and cordierite pseudomorphs in samples 8907C7 and R9828C30.

Three samples from Voksa and Sandsøya yield results consistent with a single *P–T* path. The

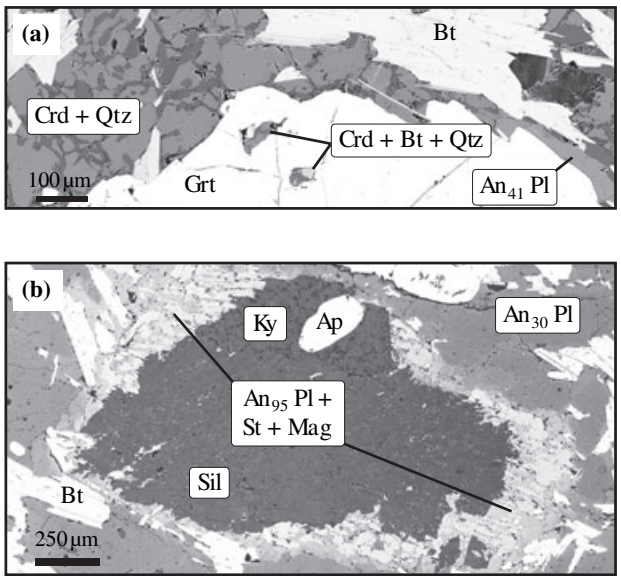

Fig. 8. Backscattered electron images of replacement reactions in sample R9828C30. (a) Intergrowth of cordierite + quartz between biotite and garnet, and cordierite + biotite + quartz inclusions within garnet. (b) Two-stage replacement of kyanite, first to sillimanite and subsequently to intergrowth of staurolite + anorthite + magnetite. Sharp gradients in anorthite content of plagioclase are preserved.

© 2005 Blackwell Publishing Ltd

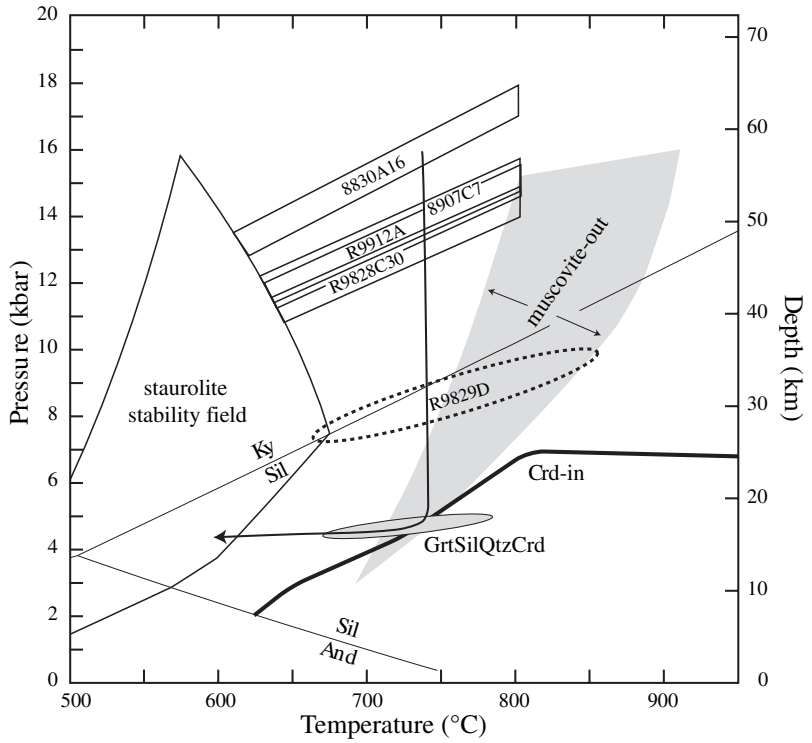

Fig. 9. Inferred *P–T* evolution of metapelite samples (arrowed). *P–T* estimates from THERMOCALC (1σ uncertainties). Boxes show garnet–kyanite–quartz–plagioclase (GASP) barometry from garnet and plagioclase core compositions. Grt-Sil-Qtz-Crd ellipse shows equilibrium among garnet, sillimanite, cordierite and quartz, sample R9828C30. R9829D ellipse shows equilibrium among garnet, muscovite, biotite and plagioclase, achieved in the Proterozoic. Muscovite dehydration region from Castro *et al.* (2000) and Patiño Douce & McCarthy (1998). Cordierite-in reaction for average pelite from White *et al.* (2001). Staurolite field from 3/2001 version of GIBBS program of Spear & Menard (1989), using Holland & Powell (1998) database.

Remøyholmen sample yields a considerably higher peak pressure (Fig. 9); but, as these peak pressures are minima, all four samples might have followed the same path. The presence of cordierite and pinite on Voksa and Sandsøya but not on Remøyholmen may have arisen from hotter and/or lower-pressure overprinting in the former location, bulk compositional differences, or kinetic differences. The simplest interpretation is that these four samples represent a single exhumation path (Fig. 9).

PROTEROZOIC Sm/Nd GARNET AGE FROM SANDSØYA

In an attempt to determine the age of the allochthon metamorphism, Sm/Nd garnet–whole rock dating was applied to a 15-cm diameter garnet from a garnet–biotite amphibolite on SE Sandsøya (R9829D, Fig. 4), with the hope that such a large garnet would preserve information about multiple stages of high-temperature metamorphism. The garnet is large enough to rule out diffusional modification of the garnet core; from core to rim it shows a weak Mn bell, constant Ca, and a minor change in Mg# from 16.6 to 17.6 (Fig. 5c). These features imply garnet growth at nearly constant pressure and temperature – if the garnet had been diffusionally modified following growth zoning, it should have sharper gradients in Ca and Mg than in Mn. The garnet has abundant inclusions of quartz, orthoclase, biotite, ilmenite and rutile; ferrotschermakite, plagioclase and muscovite are rare. Conditions of 8.6 ± 1.1 kbar and 759 ± 77 °C are estimated from garnet–biotite–muscovite–plagioclase barometry and garnet–biotite thermometry, using the compositions of the biotite and muscovite inclusions (Table 2, Fig. 9).

The analytical techniques used for the Sm and Nd isotopic measurements are described in Ducea *et al.* (2002). The estimated 2σ analytical uncertainties are: $^{147}Sm/^{144}Nd = 0.4\%$ and $^{143}Nd/^{144}Nd = 0.001$–$0.0015\%$. Garnet–whole-rock Sm/Nd ages of 992 ± 5 and 894 ± 7 Ma were obtained for the garnet core and rim, respectively (Table 3). The garnet rim sample included material several millimetres from the actual rim, and the rim age could thus represent a mixture. The major element zoning implies that these ages reflect growth during a late Proterozoic upper amphibolite facies metamorphism and the absence of a Caledonian rim age implies that there was no garnet

Table 3. Sm–Nd isotope data, garnet core and rim and whole-rock, R9828D, garnet amphibolite, NE Sandsøya [0317667, 6906637].

Fraction	Sm (ppm)	Nd (ppm)	$^{147}Sm/^{144}Nd^*$ ($\pm 2\sigma$)†	Age ($\pm 2\sigma$)‡
Garnet core	1.87	1.43	0.516175 ± 7	
Garnet rim	1.47	2.14	0.513545 ± 8	894 ± 7
Whole-rock	2.40	15.33	0.511769 ± 5	992 ± 5

*Parent–daughter ratios are precise to *c.* 0.4%.
†$^{143}Nd/^{144}Nd$ normalized to $^{146}Nd/^{144}Nd = 0.7219$. Errors refer to last digit. Replicate analyses of LaJolla Nd standard measured during the course of this study yielded $^{143}Nd/^{144}Nd = 0.511852 \pm 0.000008$.
‡Age errors are analytical only; ages are two-point isochrons.

© 2005 Blackwell Publishing Ltd

growth during the amphibolite-facies metamorphism discussed in the previous and next sections.

$^{40}Ar/^{39}Ar$ GEOCHRONOLOGY

The age of the peak UHP metamorphism in the area of Fig. 1 is best constrained by Sm/Nd three-point mineral–whole-rock isochron ages of 410 ± 16 and 408.3 ± 6.7 Ma (2σ) from eclogites at Flemsøya (Mørk & Mearns, 1986) and Saltaneset (Carswell *et al.*, 2003a), respectively (Fig. 1). These ages are supported by a prograde monazite $^{206}Pb/^{238}U$ age of 415 ± 7 Ma from a UHP gneiss at Fjørtoft (Terry *et al.*, 2000b). A slightly younger age of 405–400 Ma is implied by U/Pb zircon results from several HP and UHP eclogites from Nordfjord to Hareidlandet – including Verpeneset and Ulsteinvik (Carswell *et al.*, 2003b; Root *et al.*, 2004). Important constraints on the exhumation history of the study area come from coupling these high-T chronometers with $^{40}Ar/^{39}Ar$ geochronology.

All $^{40}Ar/^{39}Ar$ analyses employed incremental heating in a resistance furnace. Sample 93FJ39 was crushed, sieved to fraction size 250–350 μm, and subjected to magnetic separation and hand-picking prior to analysis at the Norwegian Geological Survey; all others were analysed at the Laboratory for Argon Geochronology at UCSB (Table 4; Figs 10 & 11) using analytical techniques following Calvert *et al.* (1999). Mineral separates analysed at UCSB were picked from coarsely crushed centimetre- to decimetre-sized samples not subjected to physical homogenization. Weighted mean plateau ages (WMPA) were calculated from consecutive step ages that make up >50% of the released ^{39}Ar and are statistically equivalent at the 95% confidence interval. Weighted mean ages (WMA) were calculated from consecutive step ages that are not statistically equivalent at the 95% confidence interval, but for which a part of the spectrum is not hump shaped, saddle shaped, crank-shaft shaped, or composed of serially increasing or decreasing step ages; these 'non-flat' spectrum types often indicate excess Ar, *in vacuo* degassing of more than one mineral or domain, or recoil of $^{39}Ar^{K}$ (see Discussion in Hacker *et al.*, 2003). All $^{40}Ar/^{39}Ar$ data are given in Table S1. Isochrons were calculated using a York (1969) fit to contiguous ratios not corrected for atmospheric Ar, and evaluate validity of the isochron using the expectation values for the mean-squared weighted deviation (MSWD) defined by Wendt & Carl (1991).

Eight K-white mica and two biotite from the area in Fig. 1, and two each of hornblende and biotite from *c.* 125–150 km farther NE at Enge and Aspøy (inset, Fig. 1), were analysed in this study. Five K-feldspar from this area reported by (Hacker *et al.*, 2004) are included in Fig. 1. All these $^{40}Ar/^{39}Ar$ samples come from undeformed late amphibolite facies veins, except for phengite from a UHP eclogite at Verpeneset

Table 4. Summarized $^{40}Ar/^{39}Ar$ data (2σ).

Sample	Sample description	Weight (mg)	Fusion age (Ma)	WMPA (Ma)	WMA (Ma)	Isochron age [MSWD]	$^{40}Ar/^{36}Ar$
Hbl-8814A [0477120, 7001717]	Amphibolitic margin of eclogite boudin	6.9	446.0 ± 0.8 (3.5)			**402.7 ± 8.8 (9.3) [1.2]**	13024 ± 1645
Hbl-8814B [0443406, 6984994]	Amphibolitic margin of eclogite boudin	4.3	427.2 ± 0.8 (3.4)			**402.1 ± 2.9 (4.2) [2.5]**	2304 ± 206
Bt-8814A [0477120, 7001717]	Amphibolitic margin of eclogite boudin	0.71	398.0 ± 0.8 (3.2)		**397 ± 2 (4)**	396.8 ± 1.3 (3.3) [1.9]	286 ± 20
Bt-8814B [0443406, 6984994]	Qtz–Bt–Hbl–Kfs vein, margin of eclogite boudin	0.74	393.1 ± 0.7 (3.1)		**397 ± 3 (4)**	NR	
Bt-8823B1 [035013, 694252]	Hbl–Qtz–Bt vein, margin of eclogite boudin	0.57	390.3 ± 0.7 (3.1)		**390 ± 4 (5)**	NR	
Bt-93FJ39 [036839, 695634]	Phlogopite, Vågholmen (Fjørtoft) UHP gneiss	<10	379 ± 1 (3.1)		**380 ± 3 (4)**	NR	
Ms-8828A2 [032770, 691485]	Ms–Qtz–Kfs–Bt vein, margin of eclogite boudin	0.29	381.0 ± 1.1 (3.1)	**380.1 ± 1.1 (3.1)**		379.9 ± 1.2 (3.1) [1.2]	371 ± 15
Ms-8830B2 [032795, 692008]	Qtz–Bt–Ms vein	0.50	376.2 ± 0.8 (3.0)			373.4 ± 1.0 (3.0) [0.6]	495 ± 83
Ms-8906A6 [032575, 692085]	Qtz–Bt–Ms–Grt–Kfs vein, margin of eclogite boudin	0.25	378.9 ± 1.1 (3.1)	**377.6 ± 1.1 (3.1)**	**374 ± 1 (3)**	377.4 ± 1.3 (3.2) [0.5]	364 ± 116
Ms-8907C3 [031578, 690314]	Qtz–Pl–Bt–Ms vein	0.44	385.2 ± 0.7 (3.0)		**⩽383**	382.2 ± 1.1 (3.1) [1.3]	407 ± 75
Ms-8908B2 [031692, 690498]	Qtz–Pl–Ms–Bt–Tur pegmatite	0.50	383.6 ± 0.7 (3.0)		**384 ± 1 (3)**	382.2 ± 1.0 (3.1) [1.3]	522 ± 94
Ms-8911B1 [030449, 690052]	Deformed Qtz–Kfs–Ms–Bt–Pl vein	0.70	381.3 ± 0.7 (3.0)	**379.6 ± 0.8 (3.0)**		NR	
Ms-8913A1 [030172, 689136]	Kfs–Ms vein, margin of eclogite boudin	0.35	369.5 ± 1.0 (3.0)	**369.1 ± 1.1 (3.0)**		368.9 ± 1.2 (3.0) [0.2]	344 ± 20
Ms-R9901B1 [0300567, 6869159]	Phengite, Verpeneset UHP eclogite	0.32	401.8 ± 0.8 (3.2)		**401 ± 1 (3)**	400.5 ± 0.9 (3.2) [1.6]	301 ± 22

Sample prefixes: Hbl, hornblende; Bt, biotite; Ms, white mica. Ages: WMPA, weighted mean plateau age; WMA, weighted mean age. NR, not resolvable.
Preferred ages in bold.
Second age uncertainty in parentheses includes error in decay constant and monitor age, after Renne *et al.* (1998).

© 2005 Blackwell Publishing Ltd

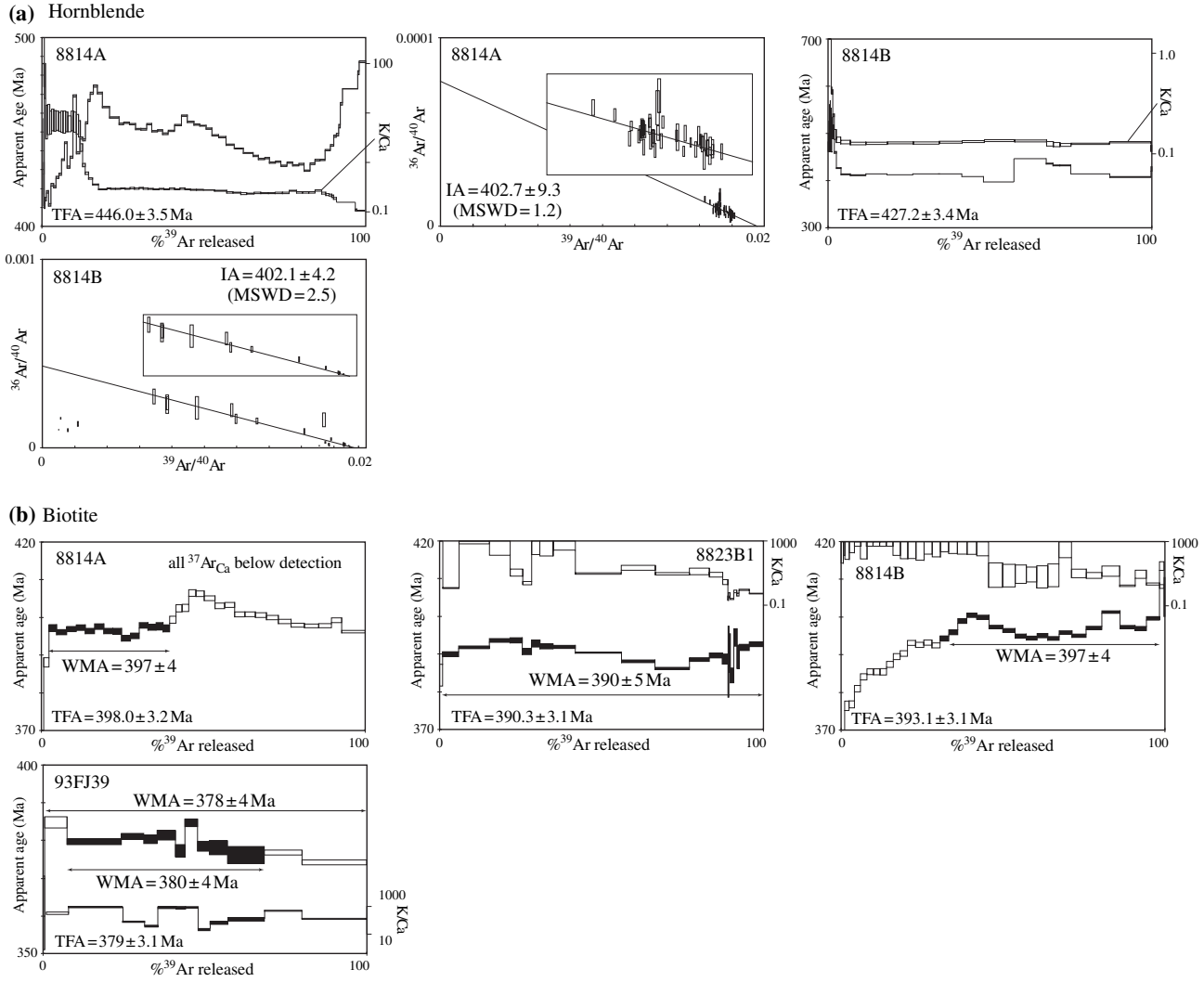

Fig. 10. (a) Hornblende $^{40}Ar/^{39}Ar$ age spectra, K/Ca spectra and inverse isochrons; see text for details of isochron regression. (b) Biotite $^{40}Ar/^{39}Ar$ age and K/Ca spectra. Quoted age uncertainties are 2σ, step age uncertainties are 1σ. WMA, weighted mean age; MSWD, mean square of weighted deviates.

(R9901B1), and biotite from an UHP gneiss at Fjørtoft (93FJ39). These veins occur in basement gneisses (8911B1, 8830B2), in allochthonous metasedimentary sequences (8907C3, 8908B2), and in the necks of eclogite boudins (8814A, 8814B, 8823B1, 8828A2, 8906A6, 8913A1). $^{40}Ar/^{39}Ar$ ages from these samples are thus post amphibolite facies cooling ages.

Amphibolitic margins to eclogite boudins at Enge and Aspøy (inset, Fig. 1) both contain hornblende with clear evidence of excess ^{40}Ar in their release spectra (Fig. 10a). Well-fit inverse isochron ages of 403 and 402 Ma are obtained for these hornblende from 75% and 41% of the ^{39}Ar released, with trapped $^{40}Ar/^{36}Ar$ ratios considerably in excess of atmospheric (Table 4). The biotite from these two samples did not yield plateaux; weighted mean ages of 397 Ma are estimated for both (Fig. 10b). Biotite samples from Vigra and Fjørtoft (Fig. 1) yielded weighted mean ages of 390 and 380 Ma, respectively, for spectra that are likely contaminated by excess ^{40}Ar (Fig. 10b). Flatter spectra were obtained from K-white mica, though most have older low-temperature step ages suggesting excess ^{40}Ar; four of eight samples yielded plateaux ages of 369, 378, 380 and 380 Ma (Fig. 11). Another three have relatively flat spectra without plateaux, and yielded weighted mean ages of 374, 384 and 401 Ma. The 401 Ma age is derived from phengite from the UHP Verpeneset eclogite, and may include excess ^{40}Ar, as it is *c.* 10 Myr older than K-white mica from the surrounding gneiss (Fig. 1). The final K-white mica sample, from Voksa, has a saddle-shaped spectrum, presumably the result of excess ^{40}Ar; a maximum age of 383 Ma is interpreted for this sample. The high-temperature step ages of five K-feldspar from the area of Fig. 1 are 380 Ma (Godøya), 370 Ma (Enge), 355 Ma (Sandsøya), 350 Ma (Aspøy), and 345 Ma

© 2005 Blackwell Publishing Ltd

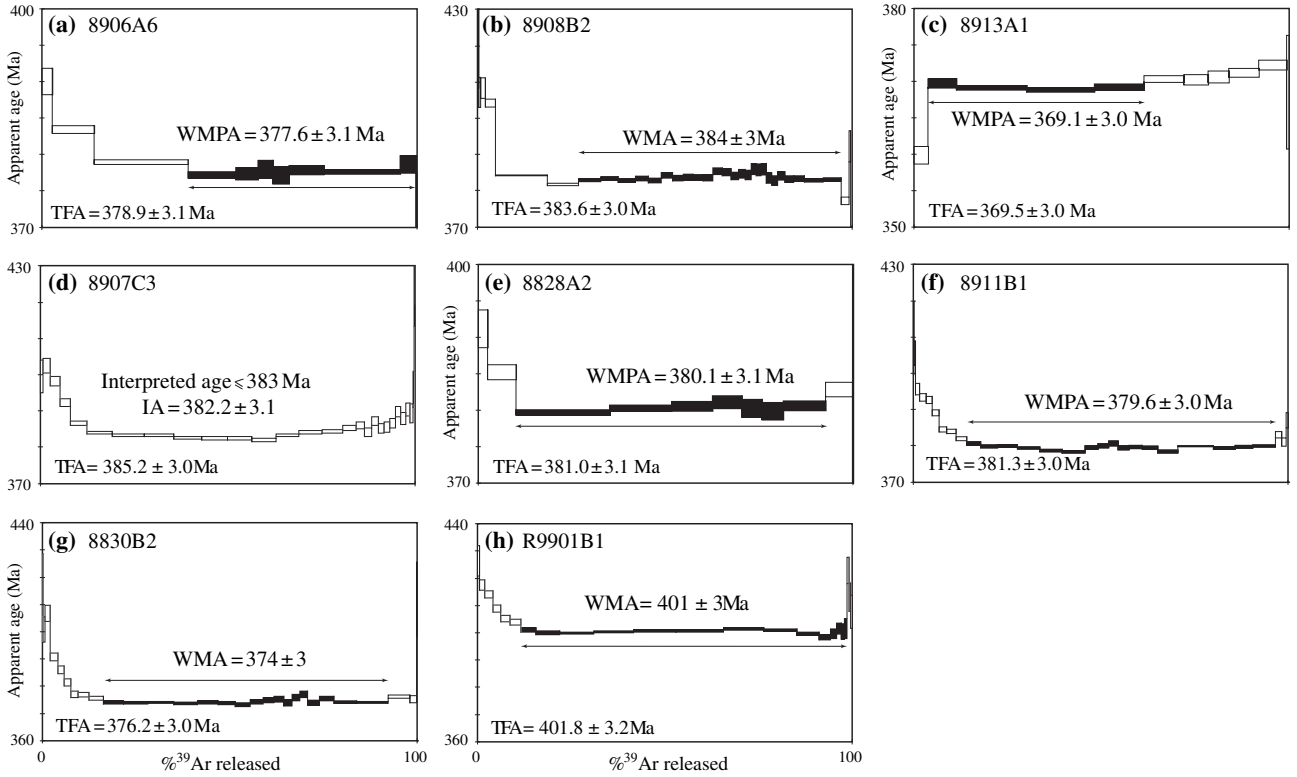

Fig. 11. K-white mica $^{40}Ar/^{39}Ar$ spectra. Quoted age uncertainties are 2σ, step age uncertainties are 1σ. None of these samples had measurable $^{37}Ar_{Ca}$. WMPA, weighted mean plateau age; WMA, weighted mean age.

(Nerlandsøya); these are interpreted to reflect closure through temperatures of *c.* 300 °C, and are in accord with the muscovite ages (Hacker *et al.*, 2004).

SIZE AND SHAPE OF THE UHP DOMAINS AND OF THE UHP TERRANE

The size and shape of the Norwegian UHP terrane can now be much more clearly defined. Our new work, in concert with other eclogite locales studied by Cuthbert *et al.* (2000); Terry *et al.* (2000a), and Terry & Robinson (2004), shows that distinct areas with UHP eclogites are separated by areas with HP eclogites (Fig. 1). Moreover, the UHP areas are characterized by younger $^{40}Ar/^{39}Ar$ ages for both white mica and K-feldspar than the HP areas (Fig. 1). Specifically, the Sorøyane UHP domain has relatively young K-white mica ages of 380–374 Ma, and the Stadlandet UHP domain has similarly young mica ages of 375–369 Ma. These contrast with older 390–380 Ma mica ages from the HP area between Hareidlandet and Fjørtoft, and with 384–380 Ma muscovite ages from the HP area between Stadlandet and Sandsøya. When combined with the $^{40}Ar/^{39}Ar$ ages of Chauvet & Dallmeyer (1992); Andersen *et al.* (1998); Walsh *et al.* (in press) and Lux (1985), and contoured, these age data reveal a significant, previously unknown feature: the areas with the young $^{40}Ar/^{39}Ar$ ages and the areas with the UHP eclogites approximately coincide (Fig. 1). Specifically, K-white mica *c.* 380 and 390 Ma chrontours and associated UHP occurrences define three distinct UHP domains: a Nordfjord–Stadlandet UHP domain of *c.* 2500 km^2, a Sorøyane UHP domain of *c.* 1000 km^2, and a Nordøyane UHP domain of *c.* 100 km^2. Because the UHP rocks are high-pressure rocks and have younger $^{40}Ar/^{39}Ar$ ages, they must represent deeper structural levels, whereas the surrounding HP domains with the older muscovite ages are shallower structural levels that cooled earlier. This, combined with the shape of the domains, implies that the UHP rocks occupy the cores of east-plunging antiforms (Fig. 1). Two important corollaries arise from this new observation.

(1) As demonstrated in Fig. 1, the amphibolite facies foliations on the south limb of the Nordfjord–Stadlandet antiform dip mostly southward, and those on the north limb of the antiform dip mostly northward. This observation is compatible with formation of the antiform entirely at amphibolite facies conditions, but some folding of the UHP domains might have occurred after cooling to greenschist facies temperatures of *c.* 350 °C at 380 Ma because the mica inside the UHP domains was just beginning to close to Ar loss, whereas that outside the UHP domains had begun closing 5–10 Myr earlier. Moreover, the amphibolite-facies foliations within the Sorøyane antiform do not

© 2005 Blackwell Publishing Ltd

dip consistently northward on the north limb and southward on the south limb. This implies that the UHP antiforms produced only minor tilting of the amphibolite facies fabrics and suggests that the antiforms have amplitudes of no more than a few kilometres (Fig. 1, cross-section); the minimal topography in the study area means that the amplitudes could be even smaller. This folding may have been part of the same long-term N–S shortening in western Norway (Torsvik *et al.*, 1988; Braathen, 1999) that Eide *et al.* (1999) showed continued until at least *c.* 340 Ma, because the high-*T* step age from K-feldspar inside the Sorøyane UHP domain is 345 Ma whereas those immediately south and north are older at 355 and 380 Ma. Notably, these Late Devonian–early Carboniferous folds have W-plunging axes – exhibited best by the 'Old Red Sandstone' basins and detachment faults south of the study area (Chauvet & Séranne, 1994) – implying that the E-plunging UHP 'antiforms' may in fact be domes produced by the superposition of young W-plunging folds on older E-plunging folds.

(2) The three UHP domains are probably connected at depth and define a UHP terrane with minimum average dimensions of *c.* 165 × 50 × 5 km. The UHP terrane likely continues in the subsurface north, east and south of the exposed area. The fact that the UHP terrane *underlies* high-pressure rocks over a large region has significant implications for the exhumation of the UHP rocks. First, this means that the lower contact of the UHP rocks is not exposed, and therefore one will never know (i) the thickness of the UHP rocks, (ii) whether the base of the UHP rocks is tectonic or an undisturbed Moho, and (iii) the history of any such basal shear zone. Second, the upper contact of the UHP rocks *is* exposed. That it can be defined (so far) only by using petrology and chronology – and not by mapping structures in the field – requires that the upper contact of the UHP rocks formed prior to the final granulite facies metamorphism, which must have annealed any shear zone along the contact. This suggests that, like the lower contact, kinematic interpretation of the upper contact based on the observation of field structures may be limited to special occurrences (e.g. Terry & Robinson, 2004). The limited intermixing of UHP and HP eclogites (except in the area between Flatraket and Verpeneset) implies that the upper contact of the UHP rocks has been disturbed no more than a few kilometres by the amphibolite-facies folding.

(ULTRA)HIGH-PRESSURE METAMORPHISM IN THE SORØYANE

In the northern Sorøyane, UHP eclogites crop out within the allochthons and the basement. In the southern Sorøyane, HP eclogites crop out within the allochthons and the basement. This relationship is similar to that inferred for the Nordøyane (Terry *et al.*, 2000a) and Nordfjord (Young *et al.*, 2003; Walsh & Hacker, 2004) areas. The presence of allochthons with UHP eclogites overlying basement with UHP eclogites, and allochthons with HP eclogites overlying basement with HP eclogites, requires that the allochthons were emplaced onto the Baltica margin prior to subduction of both into the mantle. The ≥12–17 kbar amphibolite facies metamorphism in the Sorøyane allochthons reveals that the next event was recrystallization at lower crustal depths of 45–60 km or more. This 'event' is inferred to be merely an arbitrary part of the post-(U)HP decompression path, recorded simply because further retrogression required hydration and the needed fluids were not available (e.g. Proyer, 2003). That this metamorphism may have extended over the entire area of Fig. 1 is suggested by similar pressures and temperatures (785–850 °C, 16–17 kbar; our recalculations) recorded by two granulites and an eclogite in the Enge–Aspøy area (inset, Fig. 1) (Krogh, 1980). The subsequent granulite facies overprint in the Sorøyane occurred at significantly shallower, upper crustal, depths of *c.* 20 km. The consistently high, *c.* 750 °C decompression path, starting from the 32-kbar (U)HP metamorphism, passing through the ≥12–17 kbar amphibolite facies metamorphism, and ending with the low-pressure granulite facies metamorphism, suggests isothermal decompression.

This interpretation is supported by the narrow time interval between eclogite facies recrystallization and the retention of Ar in hornblende and muscovite. If the eclogites at Enge and Aspøy were at eclogite facies temperatures typical of the WGR (e.g. 700–800 °C, Cuthbert *et al.*, 2000) at 410–407 Ma (references cited earlier), they cooled to hornblende closure at 403–402 Ma at a rate of *c.* 30 °C Myr^{-1}. Hornblende and biotite ages at these localities differ by only 5 Myr, implying cooling rates of *c.* 50 °C Myr^{-1} (best viewed as maxima given the possibility of excess ^{40}Ar in the biotite) from *c.* 550 to 300 °C (Fig. 10b). On Fjørtoft, a minimum cooling rate of 13 °C Myr^{-1} is derived from the prograde 415 ± 7 Ma monazite (Terry *et al.*, 2000b) in a rock that experienced a peak temperature of 820 °C (Terry *et al.*, 2000a), and from our biotite age of 380 ± 4 Ma. In the Sorøyane UHP domain, a cooling rate of 13–20 °C Myr^{-1} from 795 °C (e.g. Furøya) to 400 °C is derived from the UHP zircon (re)crystallization ages of three eclogite samples at 405–400 Ma (Carswell *et al.*, 2003b; Root *et al.*, 2004) combined with white mica closure at 380–374 Ma. A 20–30 °C Myr^{-1} cooling rate is implied for the Nordfjord area by the 10–15 Myr difference between the 405–400 Ma U/Pb zircon ages for the 700 °C Flatraket (Cuthbert *et al.*, 2000) and Verpeneset (Root *et al.*, 2004) eclogites and the *c.* 390 Ma $^{40}Ar/^{39}Ar$ muscovite ages along Nordfjord (Andersen *et al.*, 1998).

Thus, rocks in the area of Fig. 1 decompressed from ultrahigh pressures to 5 kbar (*c.* 17–20 km depth) after 410–407 Ma but before 403–402 Ma, all the while maintaining elevated temperatures of *c.* 750 °C. Such profound, rapid decompression at constant tempera-

© 2005 Blackwell Publishing Ltd

ture implies adiabatic exhumation. In principle, the UHP rocks need not have decompressed isothermally, but could have cooled and then been reheated at 20 km depth by magmatism that advected heat into the crust, but the paucity of Caledonian plutons within the WGR renders this scenario unlikely. More probable is that the exhumed UHP material was of sufficient size and rose through sufficiently warm material that conductive cooling was inhibited.

This possibility is evaluated using a simple one-dimensional transient heat flow model that uses the alternating-direction, implicit, finite-difference method (Hacker, 1990). The model uses standard physical parameters (Table 5), and is started by placing an 800 °C 10-, 20- or 30-km thick layer at 100 km depth within a column of specified thermal gradient. A constant exhumation rate of 10 km Myr^{-1} is applied to bring the UHP rocks from 100 to 20 km in 8 Myr and explore the implications of varying the vertical thermal gradient of the medium through which the UHP body rises, and of varying the diameter of the UHP body. The results (Fig. 12) are qualitative as expected, but instructional. If the model UHP body is too thin or rises through a thermal gradient that is too hot, the entire body reaches temperatures in excess of 900 °C (lower right part of Fig. 12). Geologically, such a scenario is equivalent to the WGR UHP rocks attempting to rise through the overlying mantle wedge, but temperatures of 900 °C are not supported by the rock record. If a small model UHP body rises through a thermal gradient that is too cold, the entire body 'freezes' below 700 °C before reaching depths as shallow as 30 km (left side of Fig. 12). Such a scenario is equivalent to a thin piece of the WGR UHP rocks attempting to rise up the subduction channel. If the model UHP body is too thin, the entire body 'freezes' below 700 °C before reaching shallow enough depths, regardless of the thermal gradient (bottom part of Fig. 12). Model UHP bodies that are 20+ km thick and rise through intermediate thermal gradients – as would prevail within the lithospheric section of the mantle wedge immediately above the subducting plate – reach depths <30 km with 700 °C temperatures remaining in the core of the body (upper right part of Fig. 12).

Table 5. Parameters for thermal models.

Height (km)	150
Node spacing (km)	1
Thermal diffusivity ($m^2\ s^{-1}$)	1.00E−06
Thermal conductivity ($W\ mK^{-1}$)	2.5
Surface temperature (°C)	0
Asthenosphere temperature (°C)	1325
Radiogenic heat production ($\mu W\ m^{-3}$)	2.2
Length scale for same (km)	10.1
Mantle heat flow ($mW\ m^{-2}$)	17–25
Basal heat flow ($mW\ m^{-2}$)	50
Time step size (Myr)	0.01
Erosion rate (mm a^{-1} or km Myr^{-1})	0
Exhumation rate (mm a^{-1} or km Myr^{-1})	10

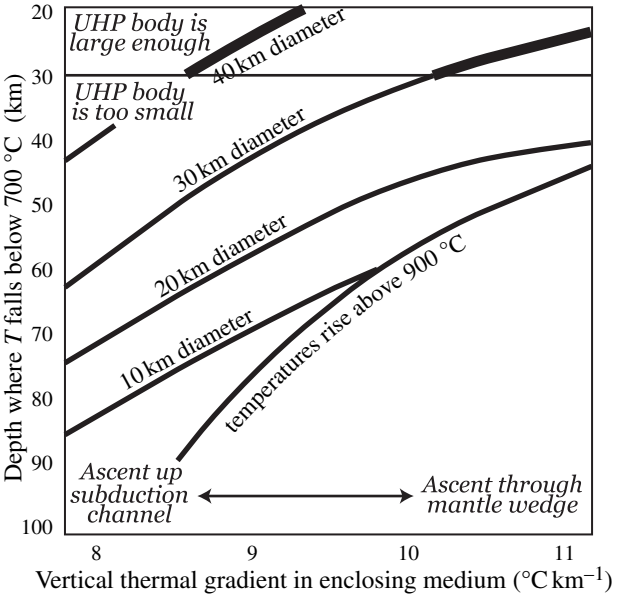

Fig. 12. Thermal modelling suggests that the UHP mass in the Sorøyane could have risen adiabatically from mantle depths through thermal gradients of 8–11 °C km^{-1} at 10 km Myr^{-1} if it was ≥30 km thick.

Very thick model UHP bodies (greater than *c.* 40 km) can also reach depths of 20 km with undisturbed 700 °C temperatures even if they rise through the cold thermal gradients typical of subduction channels (upper left part of Fig. 12). This simple modelling suggests that the UHP rocks in the Sorøyane could have risen adiabatically from mantle depths if they were 30 km thick.

The arrival of such hot material at a mid-crustal depth of *c.* 20 km established a geothermal gradient equivalent to the modern Basin-and-Range province – several hundred degrees higher than normal for continental crust (Sclater *et al.*, 1980). It was followed by rather rapid cooling to 400 °C by 397–380 Ma – the thermochronologic data by themselves suggest cooling rates of 30–50 °C Myr^{-1}, but this is a minimum because no cooling occurred during the exhumation from (U)HP depths to *c.* 20 km (5 kbar). Such rapid cooling to 400 °C cannot have occurred through passive conduction in a Basin-and-Range type thermal gradient, but is compatible with juxtaposition against cooler rocks via active exhumation of the type discussed by, for example, Andersen (1998).

CONCLUSIONS

Identification of new UHP and HP eclogite localities within the Sorøyane of the Western Gneiss Region delineates three discrete, *c.* 2500 km^2 to *c.* 100 km^2, ultrahigh-pressure (UHP) domains separated by distinctly lower pressure eclogite facies rocks. The UHP and HP domains are both composed of eclogite bearing orthogneiss basement overlain by eclogite-bearing

© 2005 Blackwell Publishing Ltd

allochthons, requiring that allochthon emplacement predates the UHP–HP metamorphism. New $^{40}Ar/^{39}Ar$ mica and K-feldspar ages reveal that the UHP domains are late, large-amplitude, regional antiforms formed at least partly at greenschist facies conditions. If the UHP culminations are part of a continuous sheet at depth, the entire UHP terrane has minimum dimensions of *c.* 165 × 50 × 5 km.

Near-isothermal decompression following (U)HP metamorphism is recorded in allochthon metapelites, which underwent upper amphibolite facies recrystallization at 12–17 kbar and *c.* 750 °C, followed by a low-pressure granulite facies metamorphism at *c.* 5 kbar and *c.* 750 °C. $^{40}Ar/^{39}Ar$ hornblende ages of 402 Ma constrain the duration of this marked decompression event to a few million years. Thermal modelling suggests that the rapid and consistently hot exhumation requires a UHP body with minimum dimensions of 20–30 km.

ACKNOWLEDGEMENTS

Funding sources for this project include NSF grant EAR-9814889, Sigma Xi, the American Federation of Mineralogical Societies, and the Department of Geological Sciences at UCSB. In addition, the aid of T. Andersen (University of Oslo) is greatly appreciated. W. Dollase and S. Harley contributed by email to our understanding of pinite. Reviews by R. Klemd and W. Hames are gratefully acknowledged.

SUPPLEMENTARY MATERIAL

The following material is available from http://www.blackwellpublishing.com/products/journals/suppmat/JMG/JMG561/JMG561sm.htm: **Table S1**. All the $^{40/39}Ar$ data derived from $^{40}Ar/^{39}Ar$ geochronology.

REFERENCES

Andersen, T.B., 1998. Extensional tectonics in the Caledonides of southern Norway, an overview. *Tectonophysics*, **285,** 333–351.

Andersen, T.B., Berry, H.B., IV, Lux, D.R. & Andresen, A., 1998. The tectonic significance of pre-Scandian $^{40}Ar/^{39}Ar$ phengite cooling ages in the Caledonides of western Norway. *Journal of the Geological Society, London*, **155,** 297–309.

Braathen, A., 1999. Kinematics of post-Caledonian polyphase brittle faulting in the Sunnfjord region, western Norway. *Tectonophysics*, **302,** 99–121.

Bryhni, I., 1989. Status of the supracrustal rocks in the Western Gneiss Region, S. Norway. In: *The Caledonide Geology of Scandinavia* (ed Gayer, R.A.), pp. 221–228, Graham and Trotman, London, UK.

Calvert, A.T., Gans, P.B. & Amato, J.M., 1999. Diapiric ascent and cooling of a sillimanite gneiss dome revealed by $^{40}Ar/^{39}Ar$ thermochronology: the Kigluaik Mountains, Seward Peninsula, Alaska. In: *Exhumation Processes: Normal Faulting, Ductile Flow, and Erosion* (eds Ring, U., Brandon, M.T., Lister, G. & Willett, S.), pp. 205–232, Geological Society of London, London, UK.

Carswell, D.A., Brueckner, H.K., Cuthbert, S.J., Mehta, K. & O'Brien, P.J., 2003a. The timing of stabilisation and the exhumation rate for ultra-high pressure rocks in the Western Gneiss Region of Norway. *Journal of Metamorphic Geology*, **21,** 601–612.

Carswell, D.A., Tucker, R.D., O'Brien, P.J. & Krogh, T.E., 2003b. Coesite inclusions and the U/Pb age of zircons from the Hareidland Eclogite in the Western Gneiss Region of Norway. *Lithos*, **67,** 181–190.

Castro, A., Corretgé, L.G., El-Biad, M., El-Hmidi, H., Fernández, C. & Patiño Douce, A.E., 2000. Experimental constraints on Hercynian anatexis in the Iberian Massif, Spain. *Journal of Petrology*, **41,** 1471–1488.

Chauvet, A. & Dallmeyer, R.D., 1992. $^{40}Ar/^{39}Ar$ mineral dates related to Devonian extension in the southwestern Scandinavian Caledonides. *Tectonophysics*, **210,** 155–177.

Chauvet, A. & Séranne, M., 1994. Extension-parallel folding in the Scandinavian Caledonides: implications for late-orogenic processes. *Tectonophysics*, **238,** 31–54.

Corfu, F., 1980. U–Pb and Rb–Sr systematics in a polyorogenic segment of the Precambrian shield, central southern Norway. *Lithos*, **13,** 305–323.

Cuthbert, S.J., Carswell, D.A., Krogh–Ravna, E.J. & Wain, A., 2000. Eclogites and eclogites in the Western Gneiss Region, Norwegian Caledonides. *Lithos*, **52,** 165–195.

Ducea, M., Sen, G., Eiler, J. & Fimbres, J., 2002. Melt depletion and subsequent metasomatism in the shallow mantle beneath Koolau volcano, Oahu (Hawaii). *Geochemistry Geophysics Geosystems*, **3,** 1015. DOI: 10.1029/2001GC000184.

Eide, E., Torsvik, T.H., Andersen, T.B. & Arnaud, N.O., 1999. Early Carboniferous unroofing in western Norway and alkali feldspar thermochronology. *Journal of Geology*, **107,** 353–374.

Gjelsvik, T., 1951. Oversikt over bergartene på Sunnmøre og tilgrensende deler av Nordfjord. (eds. Gjelsvik, T. & Gleditsch, Chr. C.), *Norges Geologiske Undersøkelse*, **179,** 1–45.

Hacker, B.R., 1990. Simulation of the metamorphic and deformational history of the metamorphic sole of the Oman ophiolite. *Journal of Geophysical Research*, **95,** 4895–4907.

Hacker, B.R., Calvert, A.T., Zhang, R.Y., Ernst, W.G. & Liou, J.G., 2003. Ultrarapid exhumation of ultrahigh-pressure diamond-bearing metasedimentary rocks of the Kokchetav Massif, Kazakhstan? *Lithos*, **70,** 61–75.

Hacker, B.R., Root, D.B., Walsh, E.O. *et al.*, 2004. Formation and exhumation of the Western Gneiss Region ultrahigh-pressure terrane: geochronology, structural geology, and petrology. *Geological Society of America Abstracts with Program*, **36,** 533.

Hernes, I., 1956. The Surnadal syncline, central Norway. *Norsk Geologisk Tidsskrift*, **36,** 25–36.

Holland, T.J.B. & Powell, R., 1998. An internally consistent thermodynamic data set for phases of petrological interest. *Journal of Metamorphic Geology*, **16,** 309–343.

Kohn, M.J. & Spear, F.S., 2000. Retrograde net transfer reaction insurance for pressure–temperature estimates. *Geology*, **28,** 1127–1130.

Krabbendam, M. & Wain, A., 1997. Late-Caledonian structures, differential retrogression and structural position of (ultra)-high-pressure rocks in the Nordfjord–Stadlandet area, Western Gneiss Region. *Norges Geologiske Undersøkelse Bulletin*, **432,** 127–139.

Krogh, E.J., 1980. Compatible *P–T* conditions for eclogites and surrounding gneisses in the Kristiansund area, western Norway. *Contributions to Mineralogy and Petrology*, **75,** 387–393.

Lutro, Ø. & Thorsnes, T., 1990. FOSNAVÅG. In: *Berggrunnskart 1119 IV*. Norges geologiske undersøkelse, Trondheim.

Lux, D.R., 1985. K/Ar ages from the Basal Gneiss Region, Stadlandet area, Western Norway. *Norsk Geologisk Tidsskrift*, **65,** 277–286.

Mørk, M.B.E. & Mearns, E.W., 1986. Sm–Nd isotopic systematics of a gabbro–eclogite transition. *Lithos*, **19,** 255–267.

© 2005 Blackwell Publishing Ltd

Mysen, B.O. & Heier, K.S., 1972. Petrogenesis of eclogites in high grade metamorphic gneisses, exemplified by the Hareidland eclogite, western Norway. *Contributions to Mineralogy and Petrology*, **36,** 73–94.

Patiño Douce, A.E. & McCarthy, T.C., 1998. Melting of crustal rocks during continental collision and subduction. In: *When Continents Collide: Geodynamics and Geochemistry of Ultrahigh-pressure Rocks* (eds Hacker, B.R. & Liou, J.G.), pp. 27–55, Kluwer Academic Publishers, Dordrecht.

Powell, R., Holland, T.J.B. & Worley, B., 1998. Calculating phase diagrams involving solid solutions via non-linear equations, with examples using THERMOCALC. *Journal of Metamorphic Geology*, **16,** 577–588.

Proyer, A., 2003. The preservation of high-pressure rocks during exhumation: metagranites and metapelites. *Lithos*, **70,** 183–194.

Renne, P.R., Swisher, C.C., Deino, A.L., Karner, D.B., Owens, T.L. & DePaolo, D.J., 1998. Intercalibration of standards, absolute ages and uncertainties in $^{40}Ar/^{39}Ar$ dating. *Chemical Geology*, **145,** 117–152.

Rickard, M.J., 1985. The Surnadal synform and basement gneisses in the Surnadal–Sunndal district of Norway. In: *The Caledonide Orogen–Scandinavia and Related Areas* (eds. Gee, D.G. & Sturt, B.A.), pp. 485–497, John Wiley & Sons, Chichester, UK.

Robinson, P., 1995. Extension of Trollheimen tectono-stratigraphic sequence in deep synclines near Molde and Brattvåg, Western Gneiss Region, southern Norway. *Norsk Geologisk Tidsskrift*, **75,** 181–198.

Root, D.B., Hacker, B.R., Mattinson, J.M. & Wooden, J.L., 2004. Zircon geochronology and ca. 400 Ma exhumation of Norwegian ultrahigh-pressure rocks: an ion microprobe and chemical abrasion study. *Earth and Planetary Science Letters*, **228,** 325–341.

Schärer, U., 1980. U–Pb and Rb–Sr dating of a polymetamorphic nappe terrain: the Caledonian Jotun Nappe, southern Norway. *Earth and Planetary Science Letters*, **49,** 205–218.

Schouenborg, B.E., 1988. U/Pb–zircon datings of Caledonian cover rocks and cover-basement contacts, northern Vestranden, central Norway. *Norsk Geologisk Tidsskrift*, **68,** 75–87.

Sclater, J.G., Jaupart, C. & Galson, D., 1980. The heat flow through oceanic and continental crust and the heat loss of the Earth. *Reviews of Geophysics and Space Physics*, **18,** 269–311.

Smith, D.C., 1984. Coesite in clinopyroxene in the Caledonides and its implications for geodynamics. *Nature*, **310,** 641–644.

Spear, F.S. & Menard, T., 1989. Program GIBBS: a generalized Gibbs method algorithm. *American Mineralogist*, **74,** 942–943.

Terry, M.P. & Robinson, P., 2004. Geometry of eclogite-facies structural features: implications for production and exhumation of ultrahigh-pressure and high-pressure rocks, Western Gneiss Region, Norway. *Tectonics*, **23** (TC2001, DOI: 10.1029/2002TC001401).

Terry, M.P., Robinson, P. & Krogh Ravna, E.J., 2000a. Kyanite eclogite thermobarometry and evidence for thrusting of UHP over HP metamorphic rocks, Nordøyane, Western Gneiss Region, Norway. *American Mineralogist*, **85,** 1637–1650.

Terry, M.P., Robinson, P., Hamilton, M.A. & Jercinovic, M.J., 2000b. Monazite geochronology of UHP and HP metamorphism, deformation, and exhumation, Nordøyane, Western Gneiss Region, Norway. *American Mineralogist*, **85,** 1651–1664.

Torsvik, T.H., Sturt, B.A., Ramsay, D.M., Bering, D. & Fluge, P.R., 1988. Paleomagnetism, magnetic fabrics and the structural style of the Hornelen Old Red Sandstone, western Norway. *Journal of the Geological Society of London*, **145,** 413–430.

Tucker, R.D., Krogh, T.E. & Råheim, A., 1990. Proterozoic evolution and age–province boundaries in the central part of the Western Gneiss region, Norway: results of U–Pb dating of accessory minerals from Trondheimsfjord to Geiranger. In: *Mid-Proterozoic Laurentia–Baltica*. GAC Special Paper, (eds. Gower, C.F., Rivers, T. & Ryan, B.), pp. 149–173, Geological Association of Canada, St. John's (Newfoundland).

Tveten, E., Lutro, Ø. & Thorsnes, T., 1998a. ÅLESUND. In: *Geologisk kart over Noreg, berggrunskart*. Noregs Geologiske Undersøkning, Trondheim.

Tveten, E., Lutro, Ø. & Thorsnes, T., 1998b. ULSTEINVIK. In: *Geologisk kart over Noreg, berggrunskart*. Noregs Geologiske Undersøkning, Trondheim.

Wain, A., 1997. New evidence for coesite in eclogite and gneisses: Defining an ultrahigh-pressure province in the Western Gneiss region of Norway. *Geology*, **25,** 927–930.

Walsh, E.O. & Hacker, B.R., 2004. The fate of subducted continental margins: Two-stage exhumation of the high-pressure and ultrahigh-pressure Western Gneiss Region, Norway. *Journal of Metamorphic Geology*, **22,** 671–687.

Walsh, E.O., Hacker, B.R., Grove, M. & Gans, P.B., in press. Time constraints on the exhumation of (ultra)high-pressure rocks across the Western Gneiss Region, Norway. *Tectonophysics*.

Wendt, I. & Carl, C., 1991. The statistical distribution of the mean squared weighted deviation. *Chemical Geology*, **86,** 275–285.

White, R.W., Powell, R. & Holland, T.J.B., 2001. Calculation of partial melting equilibria in the system Na_2O–CaO–K_2O–FeO–MgO–Al_2O_3–SiO_2–H_2O (NCKFMASH). *Journal of Metamorphic Geology*, **19,** 139–153.

York, D., 1969. Least squares fitting of a straight line with correlated errors. *Earth and Planetary Science Letters*, **5,** 320–324.

Young, D., Hacker, B.R., Andersen, T.B. & Gans, P.B., 2003. Exhumation of UHP rocks in western Norway: the role of the Nordfjord–Sogn Detachment Zone. *Geological Society of America Abstracts with Programs*, **35,** 28.

Received 18 June 2004; revision accepted 30 November 2004.

© 2005 Blackwell Publishing Ltd